Semnan University

Mechanics of Advanced Composite Structures

journal homepage: http://MACS.journals.semnan.ac.ir

Low-velocity Impact Response of Viscoelastic Composite Laminates Considering Large Deflection and Higher-order Shear Deformation

A. Tizfahm, M.R. Shokrgozar, A. Mozaffari*

Department of Aerospace Engineering, K. N. Toosi University of Technology, Tehran, Iran

KEYWORDS

Low velocity impact
Laminated composite
Sandwich structure
Viscoelasticity
Large deflection

ABSTRACT

This paper presents an experimentally validated finite element analysis of the low-velocity impact on viscoelastic laminates with consideration of large deflection and higher-order shear deformation effects in the time domain. The generalized Maxwell model (Wiechert) is incorporated into the FEM procedure to simulate the viscoelastic feature of the structure. In a geometrically nonlinear analysis, a displacement field considering higher-order shear deformation and large deflection of the laminate is assumed, and the finite element formulation is extracted. To evaluate the contact force, the modified Hertzian contact law is implemented into the finite element program. Numerical results including contact force output histories and deflections are then derived and compared with the experimental data. The obtained results show that the viscoelasticity effect and large deflection have a significant effect on the results, so they must be considered to gain a precise description of the low-velocity impact response. This model achieved good conformance with experimental results.

1. Introduction

Advanced composite materials are widely used in various industrial applications, such as marine, automotive, civil engineering, etc. in the last decades, they have become popular due to their high specific mechanical properties (strength and stiffness) regarding their specific weight mass and being more cost-effective compared to conventional materials. However, their impact resistance is considered as a disadvantage, especially under low-velocity impact conditions when the damage may remain undetected and invisible. These kinds of impact loadings can make a significant reduction in the mechanical properties of the material. To obtain a better mechanical model for the investigation of composite materials under impact conditions, the actual properties of composite materials must be taken into our calculation. Furthermore, based on previous studies, it is widely proved that viscoelasticity is one of the main intrinsic features of materials, which proves the time-dependency behavior of most materials. Viscoelastic features also can be observed for polymers, which are the main ingredient of most industrial composite structures.

Many researchers have studied the low-velocity impact analysis of composite laminates. Choi and Hong [1] studied the low-velocity impact response of composite laminates considering higher-order deformation and large deflection. However, viscoelasticity had not been considered. Sun et al. [2] implemented a first-order shear deformation theory that assumes the transverse shear strain must be constant. Wu and Springer [3] implemented a three-dimensional theory, although they did not consider large deflection effects. The maximum deflection of the plate under impact loading conditions is not small compared to the thickness of the composite laminate, so the large deflection effect must be regarded. Hosseini and Eipakchi [4] investigated the dynamic response of a viscoelastic beam with moderately large deflection and subjected to transverse and axial loads using first-order shear deformation theory.

* Corresponding author. Tel.: +98- 9122193128; Fax: +98-21-77791045
E-mail address: mozaffari@kntu.ac.ir

DOI: 10.22075/MACS.2021.22158.1315
Received 20-12-20; Received in revised form 21-08-03; Accepted 21-11-18

Cederbaum and Aboudi [5] studied the dynamical response of viscoelastic laminates. The Fourier transform (FFT) of the Boltzman representation of the viscoelastic phases is incorporated into a micromechanical analysis. The inversion of the response function into the time domain is performed by the Fast Fourier Transform algorithm. Eshmatov [6] has analyzed the nonlinear vibrations and dynamic stability of viscoelastic orthotropic plates. The contained models are based on the Kirchhoff–Love (K.L.) hypothesis and Reissner–Mindlin (R.M.) generalized theory. Tsai and Chang [7] developed a 2-D analytical model based on Ni-Adams and Adams-Maheri models, which were included for the calculation of the energy dissipation model. Assie et al. [8] studied the behavior of viscoelastic composites under transient load. An effective algorithm for analyzing the dynamic response of orthotropic viscoelastic composite laminates has been developed in the time domain and the integral form of the constitutive laws is exploited. The generalized Wiechert model is adopted to model the viscoelastic behavior of the structure.

According to the statements above, since there is a time-dependent behavior for polymers, several researchers have investigated the viscoelastic characterization of polymeric composites. Papanicolaou et al. [9] investigated the viscoelastic characterization of a Glass-Epoxy Composite. The goal of their work was to investigate the effect of different stress levels on the creep and recovery behavior of polymer matrix composites. Naik et al. [10] studied the micromechanical characterization of fibrous composites. An efficient computational algorithm is proposed to evaluate the viscoelastic properties of fibrous composites.

Unfortunately, few researchers have considered both the viscoelastic feature and geometrical nonlinearities of a structure. Vinogradov [11] investigated the creep phenomenon of a viscoelastic column showed that geometrically nonlinear analysis presents no infinite increase in deflection after creep buckling, which is not the case in a linear analysis. Shalev and Aboudi [12] analyzed the post-buckling behavior of viscoelastic laminated plates. The time-dependent post-buckling behavior was presented, and results based on different theories of plates were compared with one another. Marques and Creus [13] dealt with the nonlinear finite element analysis of viscoelastic composite structures considering the effect of moisture and temperature. Results show the time-dependent deflection under mechanical and hygrothermal loads. Fung et al. [14] studied the dynamic stability of a viscoelastic beam subjected to harmonic and parametric excitations simultaneously and showed a variation of stability boundaries when the nonlinear effect of deformation is included in the analysis. Ghabussi et al. [15] determined frequency characteristics of a viscoelastic graphene nanoplatelet-reinforced composite circular microplate. They presented a numerical solution for the frequency analysis of a viscoelastic GPLRC circular microplate within the framework of NSGT. Governing differential motion equations were solved using Hamilton's principle. Their results show that outer to inner radius ratio (Ro/Ri), ratios of length scale and nonlocal to thickness ($l/h\ and\ \mu = h$), and graphene nanoplatelet weight fraction (g_{GPL}) have a significant influence on the frequency characteristics of the graphene nanoplatelet composite circular microplate. Al-Furjan et al. [16] dealt with the vibrational characteristics of a laminated composite annular microplate using a non-classical continuum theory called modified couple stress theory (MCST). The structure is covered with a viscoelastic foundation that is simulated via the Kelvin-Voight model. the most impressive point of their result is that when the material length scale factor increases, the effect of C_d factor on the dynamics of the system declines. Fan and Wang [17] investigated the low-velocity impact response of a shear deformable beam laminated by carbon nanotube-reinforced composite, which is auxetic. They have shown that an auxetic beam leads to reduced elastic deformation and increased impact force than nonauxetic beams. In another research, Fan et al. [18] dealt studied the Nonlinear forced vibration of FG-GRC laminated plates resting on visco-Pasternak foundatios. They have also implemented viscosity in their analysis and observed a significance impact on the final results.

In the present study, a finite element formulation has been used to analyze the low-velocity impact response considering higher-order shear deformation theory, large deflection, and the viscoelastic effect of the laminate. Governing equations are derived from Hamilton's principle using von Karman's nonlinear theory of plates and Boltzmann's superposition principle for linear viscoelastic constitutive law. Also, the higher-order shear deformation is considered in the displacement fields. To express the viscoelastic material properties, the Wiechert model is employed for approximation. The nonlinear and hereditary type governing equations are treated with the finite element method and method of multiple scales. The verification and limitation of the present approach are discussed by comparing results with those of nonlinear elastic and linear viscoelastic analysis. The hereditary characteristics of the equations make it difficult

to decouple the flexure motion. Numerical illustrations including contact force and deflection states are shown and discussed in different.

The remainder of the paper is outlined as follows. First, a brief review of the viscoelastic model and higher order shear deformation theory finite element formulations for geometrically nonlinear analysis is introduced in Section 2. In Section 3, the solving procedure and the related flow chart are described. The results are provided in Section 4 discussed in detail to show the nonlinearities and viscoelastic effects. Finally, some conclusions are made in Section 5.

2. Mathematical Model

2.1. Viscoelastic model

Viscoelasticity is a common property of materials exhibiting both viscous and elastic characteristics when undergoing deformation. Purely elastic materials do not dissipate energy when an external load is removed. On the other hand, viscoelastic materials lose energy when a load is applied. The behavior of viscoelastic materials can be expressed by arranging springs and dampers. Some proposed models that are capable of modeling viscoelasticity, such as Kelvin, Maxwell, Standard linear solid (SLS), etc. Here, the generalized Maxwell model or Wiechert model is used (Fig. 1). In this model, relaxation does not occur at a single time. Although an increasing number of Maxwell elements leads to the real behavior of the material, three Maxwell elements were considered here [8].

$$E(t) = E_0 + \sum_{i=1}^{n} E_i e^{\frac{-t}{\lambda_i}} \tag{1}$$

Here, t is time, E_0 is the spring parallel to the Maxwell elements and λ_i is relaxation time for the ith Maxwell element and defined as [8]

$$\lambda_i = \frac{\eta_i}{E_i} \tag{2}$$

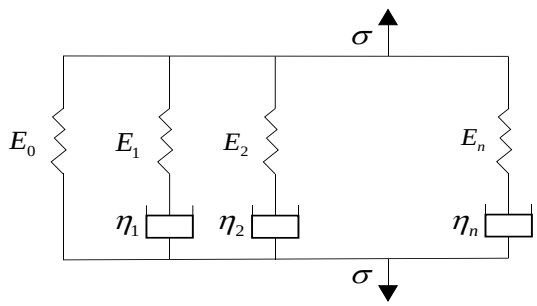

Fig. 1. Generalized Maxwell model with n Maxwell elements (Wiechert model [8])

2.1.1. Kinematics of the Maxwell model

The overall stress σ acting on the generalized model is equal to the summation of the stresses acting on the Hookean spring and the parallel Maxwell elements. Adopting the generalized Maxwell model, the stress of the material is expressed as [8]

$$\sigma(t) = E_0\varepsilon(0) + \sum_{i=1}^{n} E_i e^{\frac{-t}{\lambda_i}}\varepsilon(0) = E(t)\varepsilon(0) \tag{3}$$

where $\varepsilon(0)$ is the initial strain of the Maxwell element in its relaxation test. The stress-strain curve of the relaxation test for a Maxwell element is shown in Fig. 2.

2.1.2. Mathematical formulation

Figure 3 shows the geometric configuration of a lamina under the low-velocity impact. In this study, a higher-order displacement field is adopted to consider both membrane effects and large deflections of the lamina. Supposedly, the x-y plane coincides with the neutral plane of composite lamina whose thickness direction is oriented along the z-axis. The displacement components of the lamina are described as [1]

$$\begin{aligned} u^x(x,y,z,t) &= u(x,y,t) + z\psi^x(x,y,t) \\ &\quad + z^3\zeta^x(x,y,t) \\ u^y(x,y,z,t) &= v(x,y,t) + z\psi^y(x,y,t) \\ &\quad + z^3\zeta^y(x,y,t) \\ u^z(x,y,z,t) &= w(x,y,t) \end{aligned} \tag{4}$$

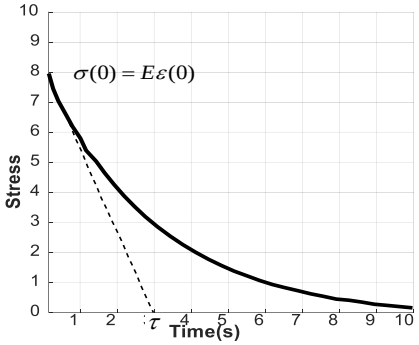

Fig. 2. Relaxation test of a Maxwell element [19]

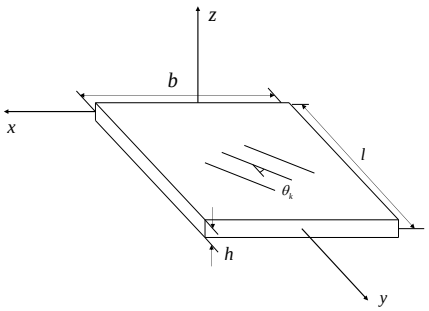

Fig. 3. The geometric configuration of a composite laminate

Here $u^x, u^y, u^z$are the displacement in the x,y,z direction, respectively; u, v, w are the displacements of the neutral plane; ψ^x,ψ^y and ζ^x,ζ^y are the first- and third-order rotations of the cross-sections normal to the x, y-axis, respectively. The strain-displacement relations developed by von Karman's large deflection theory relation to include geometric nonlinearities can be written as [1]

$$\varepsilon_1 = \frac{\partial u^x}{\partial x} + \frac{1}{2}\left(\frac{\partial u^z}{\partial x}\right)^2 = \frac{\partial u}{\partial x} + \frac{1}{2}\left(\frac{\partial w}{\partial x}\right)^2 + z\left(\frac{\partial \psi^x}{\partial x} + z^2\frac{\partial \zeta^x}{\partial x}\right)$$

$$\varepsilon_2 = \frac{\partial u^y}{\partial y} + \frac{1}{2}\left(\frac{\partial u^z}{\partial y}\right)^2 = \frac{\partial v}{\partial y} + \frac{1}{2}\left(\frac{\partial w}{\partial y}\right)^2 + z\left(\frac{\partial \psi^y}{\partial y} + z^2\frac{\partial \zeta^y}{\partial y}\right)$$

$$\varepsilon_3 = \frac{\partial u^x}{\partial y} + \frac{\partial u^y}{\partial x} + \left(\frac{\partial u^z}{\partial x}\frac{\partial u^z}{\partial y}\right) = \frac{\partial u}{\partial y} + \frac{\partial v}{\partial x} + \left(\frac{\partial w}{\partial x}\frac{\partial w}{\partial y}\right) + + z\left\{\frac{\partial \psi^x}{\partial y} + \frac{\partial \psi^y}{\partial x} + z^2\left(\frac{\partial \zeta^x}{\partial y} + \frac{\partial \zeta^y}{\partial x}\right)\right\} \quad (5)$$

$$\varepsilon_4 = \frac{\partial u^z}{\partial y} + \frac{\partial u^y}{\partial z} = \frac{\partial w}{\partial y} + \psi^y + 3z^2\zeta^y$$

$$\varepsilon_5 = \frac{\partial u^z}{\partial x} + \frac{\partial u^x}{\partial z} = \frac{\partial w}{\partial x} + \psi^x + 3z^2\zeta^x$$

where contracted notations are used for engineering strains. As the viscoelastic constitutive law, Boltzmann's superposition principle for linear viscoelastic behavior is employed. The stress-strain relation at the *k*th layer, which has the orientation angle of *k*th, is given in the hereditary type form as follows [20]:

$$\sigma_i^k(t) = \int_{0^-}^{t} \bar{Q}_{ij}^k(t-s)\dot{\varepsilon}_j^k(s)ds \quad i = 1,2,3,4,5 \quad (6)$$

Here, the repeated index stands for the summation rule and $\bar{Q}_{ij}^k(t)$ is the relaxation function at the *k*th layer referred to x-y coordinates, which are obtained from the axis transformation of the relaxation modulus $Q_{ij}(t)$ referred to the principal material axes. In terms of generalized displacements and forces, constitutive relations are written in the following form as in Cederbaum *et al.* [21]

$$\begin{Bmatrix} N_{xx} \\ N_{yy} \\ N_{xy} \\ M_{xx} \\ M_{yy} \\ M_{xy} \end{Bmatrix} = \begin{bmatrix} A_{11} & A_{12} & A_{13} & B_{11} & B_{12} & B_{13} \\ & A_{22} & A_{23} & B_{12} & B_{22} & B_{23} \\ & & A_{33} & B_{13} & B_{23} & B_{33} \\ & & & D_{11} & D_{12} & D_{13} \\ & Sym. & & & D_{22} & D_{23} \\ & & & & & D_{33} \end{bmatrix} * \begin{Bmatrix} \dot{u}_{,x} + w_{,x}\dot{w}_{,x} \\ \dot{v}_{,y} + w_{,y}\dot{w}_{,y} \\ \dot{u}_{,y} + \dot{v}_{,x} + \dot{w}_{,x}w_{,y} + w_{,x}\dot{w}_{,} \\ \dot{\psi}_{x,x} \\ \dot{\psi}_{y,y} \\ \dot{\psi}_{x,y} + \dot{\psi}_{y,x} \end{Bmatrix} \quad (7)$$

and

$$\begin{Bmatrix} Q_{yy} \\ Q_{xx} \end{Bmatrix} = \begin{bmatrix} A_{44} & A_{45} \\ A_{45} & A_{55} \end{bmatrix} * \begin{Bmatrix} \dot{\psi}_y + \dot{w}_{,y} \\ \dot{\psi}_x + \dot{w}_{,x} \end{Bmatrix}$$

In this formula, overdot stands for the time derivative, * denotes the convention operator.

Time-dependent functions $A_{ij}(t)$, $B_{ij}(t)$ and $D_{ij}(t)$ are defined by

$$(A_{ij}(t), B_{ij}(t), D_{ij}(t)) = \int_{-h/2}^{h/2} \bar{Q}_{ij}^k(t)(1, z, z^2)dz \qquad i,j = 1,2,3 \quad (8)$$

$$A_{ij}(t) = \int_{-h/2}^{h/2} \bar{Q}_{ij}^k(t)dz \qquad i,j = 4,5$$

The equations of motion are derived from the extended Hamilton's principle for the non-conservative system:

$$\int_{t_1}^{t_2} \delta K - (\delta U - \delta V)dt = 0 \quad (9)$$

where δK is the virtual kinetic energy, δU denotes the virtual strain energy and δV expresses the virtual work done by external forces respectively as are given by

$$\delta K = \int_{Area} \{I_0(\dot{u}\delta\dot{u} + \dot{v}\delta\dot{v} + \dot{w}\delta\dot{w}) + I_2(\dot{\psi}_x\delta\dot{\psi}_x + \dot{\psi}_y\delta\dot{\psi}_y\}dxdy$$

$$\delta U = \int_{Area} N_{xx}(\delta u_{,x} + w_{,x}\delta w_{,x}) + M_{xx}\delta\psi_{x,x} + N_{yy}(\delta v_{,y} + w_{,y}\delta w_{,y}) + M_{yy}\delta\psi_{yy} + N_{xy}(\delta u_{,y} + \delta v_{,x} + w_{,x}\delta w_{,y} + w_{,y}\delta w_{,x}) + M_{xy}(\delta\psi_{x,y} + \delta\psi_{y,x}) + V_x(\delta\psi_x + \delta w_{,x}) + V_y(\delta\psi_y + \delta w_{,y})dxdy \quad (10)$$

$$\delta V = \int_{Area} F\,\delta\alpha dA$$

with inertial terms I_0, I_2, resultant forces N_{ij}, V_i and moments M_{ij} for $i,j = x,y$ being defined as

$$\begin{aligned}&(I_0, I_2) = \int_{-h/2}^{h/2} \rho(1, z^2)dz\\&\left(N_{xx}, N_{yy}, N_{xy}, V_y, V_x\right)\\&= \int_{-h/2}^{h/2} \left(\sigma_1^k, \sigma_2^k, \sigma_3^k, \sigma_4^k, \sigma_5^k\right)dz\\&\left(M_{xx}, M_{yy}, M_{xy}\right) = \int_{-h/2}^{h/2} z(\sigma_1^k, \sigma_2^k, \sigma_3^k)dz\end{aligned} \tag{11}$$

Contracted notations are utilized for stress as in the case of strain. Interpolating displacement and rotation fields in terms of nodal values and substituting them into Eqs. (5), (6), and (9), one can obtain the following discretized non-linear governing equations

$$M\ddot{x} + \sum_{i=1}^{N} \int_{0^-}^{t} Q_i(t-s)K_i\dot{x}ds = F_i \tag{12}$$

Here, F is the constant force between the laminate and the projectile. x is the global nodal vector, M is the mass matrix, and K_i are the matrices that have stiffness Q_i as coefficients. Besides, contracted indices are used for relaxation moduli referred to the principal axes of the material $Q_1 = Q_{11}, Q_2 = Q_{12}, Q_3 = Q_{22}, Q_4 = Q_{33}, Q_5 = Q_{44}$ and $Q_6 = Q_{55}$. Also, $K_1, \ldots, K_4$ are transverse displacement dependent matrices, while shear deformation dependent matrices K_5 and K_6 are constant. They can be written as

$$\begin{aligned}&K_i = K_i^0 + K_i^1 + K_i^2 \qquad i = 1,\ldots,4\\&K_i = K_i^0 \qquad i = 5,6\end{aligned} \tag{13}$$

where K_i^0 is constant and K_i^1, K_i^2 are the linear and quadratic functions of transverse displacement w, respectively.

The relaxation moduli Q_{ij} referred to the principal axes of material, are expressed in terms of the Prony–Dirichlet series, which is one of the most widely used models for approximating the viscoelastic behavior of a material. Hence, neglecting the variation of temperature and moisture, any relaxation modulus can be assumed as

$$\begin{aligned}Q_i(t) = Q_i^\infty + \sum_{j=1}^{N_i} Q_i^j\, exp(-d_i^j t)\\= Q_i(0) f_i(t) \quad for\ i\\= 1,2,\ldots,6\end{aligned} \tag{14}$$

Here, N_i is the number of exponential terms required for approximation, Q_i^∞ the final stiffness of $Q_i(t)$, Q_i^j constant coefficients, d_i^j (>0) relaxation parameters, and $f_i(t)$ is the time function that yields unity at $= 0$ and characterizes the relaxation phenomenon.

2.2. Contact law

F is the contact force at the impacted point which can be determined by Hertzian contact law as below:

$$Loading: F = k\alpha^{1.5} \tag{15}$$

$$Unloading: F = F_m \left(\frac{\alpha - \alpha_0}{\alpha_m - \alpha_0}\right)^{2.5} \tag{16}$$

k is the constant coefficient in the same direction as impact loading

$$k = \frac{4}{3}\sqrt{R}\frac{1}{\left(\frac{1-\nu^2}{E}\right) + \frac{1}{E_{yy}}} \tag{17}$$

In this formula, R is the radius of the projectile, ν, and E are the Poisson's ratio and Young's modulus of the projectile, respectively. E_{yy} is the modulus of elasticity of the uppermost composite ply in the transverse direction of the fibers, i.e. E_2 which is given in Table 2. Assuming the projectile is rigid, E quantity is considered to be infinite. F_m is maximum contact force; α, $\alpha_0$and α_m are the indentation, the permanent indentation, and the maximum indentation, respectively. α_0 can be evaluated by the following equations

$$\alpha_0 = 0 \quad \text{when} \quad \alpha_m < \alpha_{cr} \tag{18}$$

$$\alpha_0 = \alpha_m \left[1 - \left(\frac{\alpha_{cr}}{\alpha_m}\right)^{0.4}\right] \ \text{when} \ \ \alpha_m \geq \alpha_{cr} \tag{19}$$

Here α_{cr} is the critical indentation and is about 0.08 mm for Glass-Epoxy composites.

To determine the contact force using Eqs. 15 and 16, the indentation, α should be computed from the displacements of the plate and the projectile.

3. Solving Procedure

The response of the projectile is assumed to be a rigid body motion. Hence its governing equation may be determined as follows

$$m\ddot{w}_I + F = 0 \tag{20}$$

Here, m and w_I are the mass and the displacement of the projectile, respectively. F is the contact force as mentioned before. To analyze the projectile response, three equations are solved simultaneously; i.e., the finite element equation of the laminate, the governing equation of the projectile, and the contact law. Hence, an iteration is needed to solve equations 12, 20, 15, and 16 for each time step. Furthermore, since equation 12 is a non-linear equation, another iteration is needed as shown in the flowchart of Fig. 4. As considerable computational effort is

needed in the non-linear impact response analysis, Akay's constant coefficient scheme is used for efficient analysis. In this scheme, the non-linear stiffness matrix in equation (12) is moved to the right-hand side of the equation and is considered as an additional equivalent force vector. Newmarks' constant acceleration method is used to solve the time-dependent equations and successive iterations have to be continued until a desired accuracy is obtained for each time step.

Since a considerable computational effort is needed in the non-linear impact response analysis, Akay's constant-coefficient [22] scheme is used for efficient analysis. Newmark's constant acceleration method is used to solve the time-dependent equations and successive iterations have to be continued until the desired accuracy is obtained for each time step.

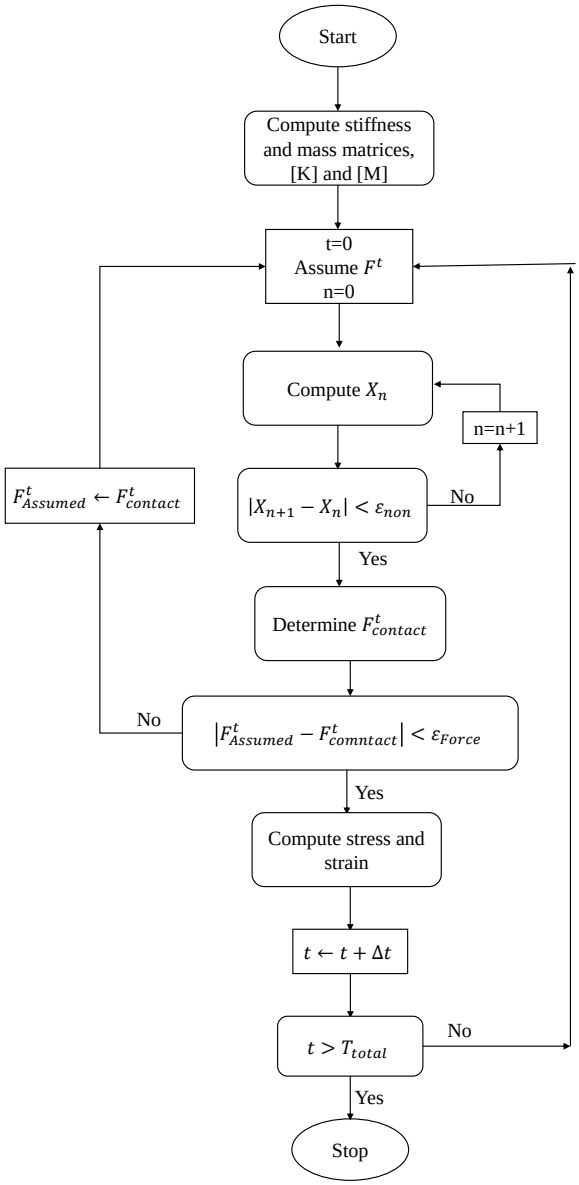

Fig. 4. Flow chart of the solving procedure

4. Results and Discussion

Two different composite laminates were opted to consider and analyze various effects on dynamical response. The first one is a 16-ply laminated Glass-Epoxy composite, and the other one is a sandwich laminate composite with 6 plies and an isotropic elastic core (Fig. 5). These two composites are subjected to a low-velocity impact with 32J initial energy (equivalent to the initial velocity of 2.83 m/s). The projectile is a semi-spherical rigid body with a diameter of 14mm and a total weight of 8kg. Geometrical dimensions and mechanical properties of composite laminates are shown in Table 1 and the relaxation test results for the determination of relaxation coefficients of Glass-Epoxy laminates in 0° and 90° orientations are shown in Table 2. Both composites have a fixed boundary condition at the upper and lower edges of surfaces. To validate the presented method used in this paper, the contact force of the presented model is compared to experimental results [23] According to the details of their experiments, composite laminates are composed of glass fiber, and epoxy resin, which is prepared by a vacuum-assisted resin injection (VARI) process. The lamina is a unidirectional glass fiber (EDW800) with a layer thickness of 0.2 mm, and a mass surface density of 200 $g/m2$. It was provided by Jiangsu Jiuding New Material Co., Ltd., Nantong, Jiangsu, P.R. China. The selected resin is an epoxy vinyl ester (VER) 411, in which the matching curing agent and accelerating agent are methyl ethyl ketone peroxide (MEKP) and dimethylaniline. It was bought from Harbin Akihito composite material Co., Ltd., Nantong, Jiangsu, P.R. China.

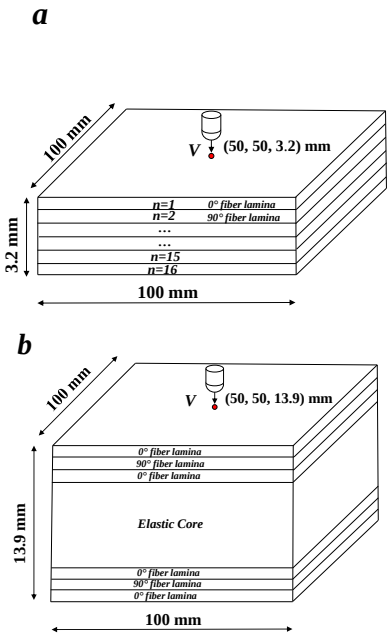

Fig. 5. (a) 16-ply Glass-Epoxy composite laminate (type 1) and (b) sandwich laminate (type 2)

Table 1. Geometrical properties of composites

	Type 1	Type 2
Length (mm)	100	100
Width (mm)	100	100
Height (mm)	3.2	13.9
Number of layers	16	6
The thickness of each ply (mm)	0.2	0.2
The thickness of the core (mm)	-	12.7
Stacking sequence	$[0/90]_8$	$[0/90/0/C]_s$
The density of core (kg/m^3)	-	110
Young's modulus of core (MPa)	-	180
Poisson's ratio of core	-	0.286

Table 2. Wiechert model coefficients determined by the relaxation test of a Glass-Epoxy composite [24]

Relaxation modulus (GPa)	0° lamina	90° lamina
E_0	21.138	6.796
E_1	0.673	0.237
E_2	0.263	0.471
E_3	0.257	0.357
E_4	0.654	0.714
Relaxation time (s)		
λ_1	30	9.6
λ_1	96	96
λ_1	996	996
λ_1	8400	8400

4.1. Representation of results for composite type 1

4.1.1. Viscoelasticity effect

A comparison between elastic and viscoelastic contact force and deflection curves is illustrated in Figs. 6 and 7, respectively. Also, the large deflection effects are considered in the results. As it can be observed, the viscoelastic response has a greater maximum contact force and is closer to the experimental results (1.3% error for viscoelastic response and 14.5% error for elastic response at the maximum contact force point), and also contact time is less than elastic response. The time of the maximum contact force is 4.5 ms in the elastic state and 4 ms in the viscoelastic state, which is very close to the experiment. This happens because Maxwell elements of the Wiechert model are parallel to the elastic spring and cause a reduction in deflection (Fig. 7). Therefore, more rigidity of the composite laminate leads to a higher contact force and smaller contact time.

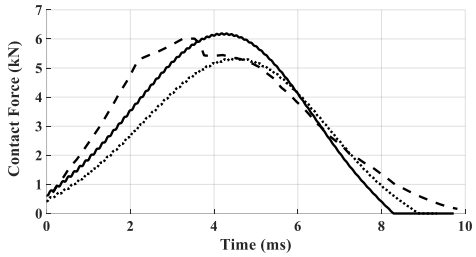

Fig. 6. Contact force versus time curves for observation of the viscoelasticity effect. Experiment (dashed), Elastic (dotted), *Viscoelastic* and large deflection (solid)

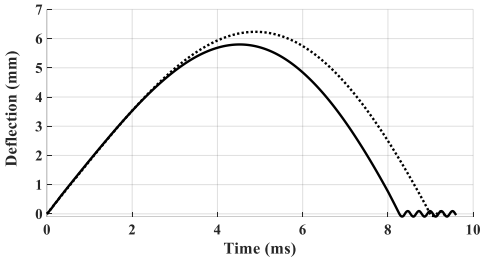

Fig. 7. Deflection versus time curves for observation of viscoelasticity effect. Elastic (dotted), Viscoelastic and large deflection (solid)

The little difference between the experiment and nonlinear and viscoelastic analytical results could be due to the following reasons: reduced composite stiffness due to impact damage and the imperfect boundary conditions in the experiment. Also, in the impact experiment, some of the impact energy is dissipated in the form of acoustic emission and damage. This type of energy dissipation has been neglected in this analysis. So, the difference between the two results is possible.

4.1.2. Large deflection effects

To show the geometry nonlinearity, large deflection effects, contact force, and deflection output histories are shown in Figs. 8 and 9, respectively. Geometrical linearity is affected by the large deflections of the composite plate. The results of Fig. 8 show, geometrical nonlinearity has a great influence on the composite impact response. So, geometrical non-linearity must be considered in the FEM analysis procedure (71% Error for a geometrically linear model).

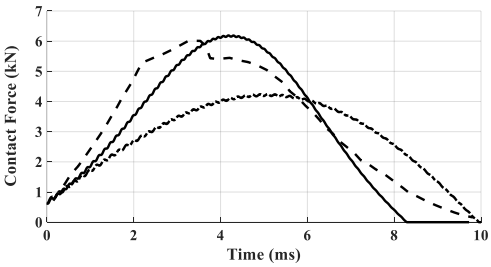

Fig. 8. Contact force versus time curves for consideration of geometrical non-linearity. Experiment (dashed), Large deflection and viscoelastic (solid), Linear geometry (dash-dotted)

Figure 9 shows the deflection histories at the impact point in two linear and nonlinear geometry. Because of large deflection effects, the non-linear deflection history is estimated to be smaller than the corresponding linear result.

4.1.3. First-order and higher-order shear deformation (FSDT and HSDT) effects

Using the two plate theories, FSDT and HSDT, consideration effects are shown in Figs. 10 and 11. It can be observed, results are not affected by considering higher-order shear deformation and they're approximately similar and there is no significant difference between the two non-linear results using the two plate theories (FSDT and HSDT)

4.1.4. Damping of vibration

In contrast to purely elastic materials, the deflection of viscoelastic materials will be damped when they are subjected to an impact loading. The damping time is affected by material characteristics that are determined by the relaxation test (table 2). This damping effect is illustrated for composite type 1 in Fig. 12. It can be observed that 0.015 seconds after getting impact, the vibration of the composite has vanished. Similar results are found in Assie's paper [8].

4.2. Representation of results for composite type 2

Since the FEM is validated in the previous section, a sandwich laminated composite is also considered to emphasize the same results. The geometrical and mechanical properties of composite type 2 are shown in tables 1 and 2, respectively. In this model, the interaction between layers and the core is ignored. Similar to composite type 1, the same factors are determined for composite type 1 (Figs. 13 and 14). Also, the damping of vibrations is shown in Fig. 15. Alternatively, it can be deduced from these figures that viscoelasticity tends to decrease the contact time and increase the peak of the contact force. It is worth mentioning that the core of the sandwich laminate is an ideal elastic foam.

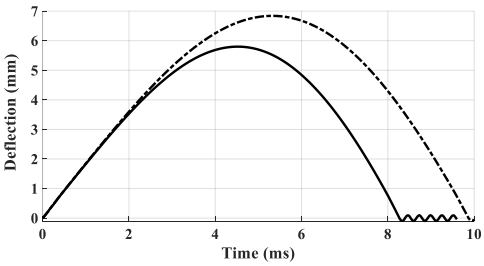

Fig. 9. Deflection versus time curves for consideration of geometrical non-linearity. Large deflection and viscoelastic (solid), Linear geometry (dash-dotted)

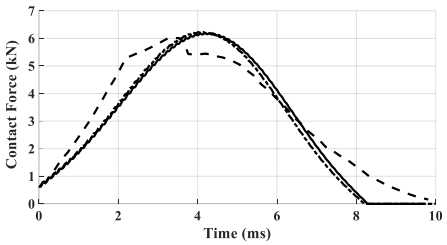

Fig. 10. Contact force versus time curves for HSDT and FSDT consideration effect. Experiment (dashed), FSDT (solid), HSDT (dash-dotted)

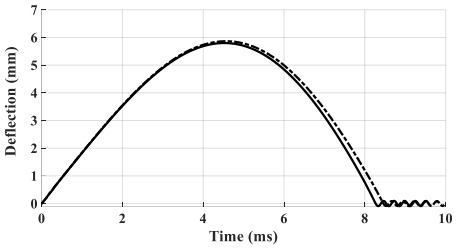

Fig. 11. Deflection versus time curves for HSDT and FSDT consideration effect. FSDT (solid), HSDT (dash-dotted)

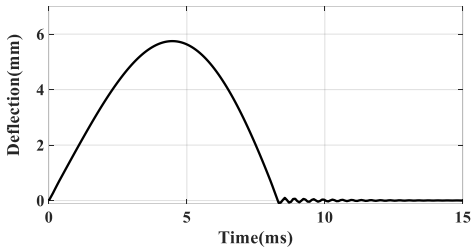

Fig. 12. The damping effect of Glass-Epoxy composite type 1

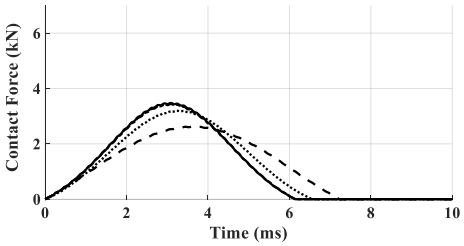

Fig. 13. Contact force versus time curves for observation of viscoelasticity, Large deflection, HSDT, and FSDT effects of sandwich laminated composite. Elastic (dotted), Viscoelastic, large deflection and FSDT (solid), Viscoelastic, large deflection and HSDT (dash-dotted), Linear geometry (dashed)

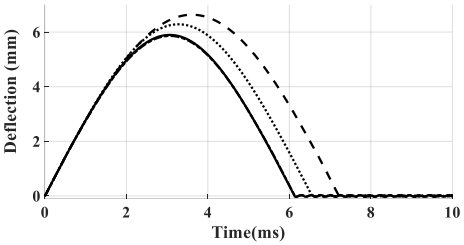

Fig. 14. Deflection versus time curves for observation of viscoelasticity, geometrical linearity, HSDT, and FSDT effects of sandwich laminated composite. Elastic (dotted), Viscoelastic, large deflection and FSDT (solid), Viscoelastic, large deflection and HSDT (dash-dotted), Linear geometry (dashed)

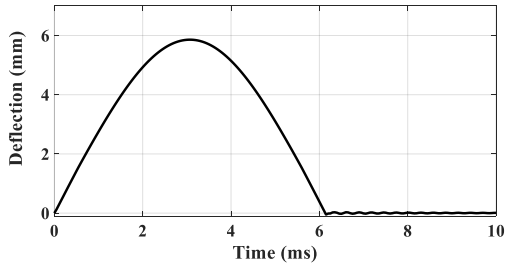

Fig. 15. The damping effect of the Glass-Epoxy sandwich composite structure type 2

Besides, these results show that in both linear and non-linear results there is barely a visible difference between the impact force histories for FSDT and HSDT responses. Consequently, considering higher-order shear deformation does not affect the global response of the sandwich, whereas considering large deflection and viscoelastic effects have a dominant influence on the impact response of the sandwich.

5. Conclusion

Due to the importance of the response of the viscoelastic composite plates under low velocity, this problem is here investigated. In this paper, the viscoelastic response of the polymeric composites was considered in geometrically nonlinear analysis of the low-velocity impact using two different theories, FSDT and HSDT. To obtain an accurate FEM modeling of laminated composites and sandwich structures, subjected to low-velocity impact conditions, three effects were investigated. As the results show, the viscoelasticity effect, besides considering large deflection, is the main feature of polymeric composites and sandwich structures and has a prominent influence on dynamical outputs. It is thoroughly demonstrated that taking these factors into account brings the final results closer to experimental ones. To sum up, the obtained conclusions include

(1) Viscoelastic behavior of a polymeric composite, besides large deflection, is the main feature that must be considered in the FEM procedure. Results depict that the viscoelastic response seems to regard a composite substantially tougher than the elastic one.
(2) The Wiechert model is very efficient to describe the viscoelastic behavior of composite plates.
(3) There is a considerable difference between geometrically linear and non-linear analysis (71% Error), which cannot be negligible.
(4) It is illustrated that considering higher-order shear deformation seems not to be noticeably effective on the final results.

All in all, it can be concluded that the viscoelasticity and large deflection effects must be taken into account simultaneously to have an accurate description of the global response of the composite laminates subjected to low-velocity impact.

Nomenclature

t	Time (s)
E	Young's modulus
λ_i	relaxation time
σ	Stress
ε	Strain
υ	Poisson's ratio
ρ	Density
η	Damper coefficient
u	displacement
ψ	First-order rotation of the cross-section
ζ	Higher-order rotation of the cross-section
Q_{ij}	Relaxation moduli
$K_i^0, K_i^1 \text{ and } K_i^2$	Linear and quadratic functions of the transverse displacement w
I	Moment of inertia
M	Mass
R	The radius of the projectile
F	Force
α	indentation
α_{cr}	Critical indentation
w_I	Displacement of the projectile

References

[1] Choi, I.H. and Hong C.S., 1994. Low-Velocity Impact Response of Composite Laminates Considering Higher-Order Shear Deformation and Large Deflection. *Mechanics of Composite Materials and Structures*, pp.37–41.
[2] Sun. C. T., and Chen, J. K., 1985. On the Impact of initially Stressed Composite Laminates. *Journal of Composite Materials*, 19(6), pp.490-504.
[3] Wu, H.Y.T. and Springer, G.S., 1988. Impact Induced Stresses, Strains, and Delaminations in Composite Plates. *Journal of Composite Materials*, 22 (6), pp.533–560.
[4] Malek-Hosseini, Z. and Eipakchi, H., 2017. An analytical procedure for dynamic response determination of a viscoelastic beam with moderately large deflection using first-order shear deformation theory. *Mechanics of Advanced Materials and Structures*, 24 (10), pp.875–884.
[5] Cederbaum, G., and Aboudi, J., 1989. Dynamic Response of Viscoelastic Laminated Plates. Journal of Sound and Vibration, 133(2), pp.225-238.
[6] Eshmatov, B.K., 2007. Nonlinear vibrations and dynamic stability of viscoelastic orthotropic rectangular plates. *Journal of*

Sound and Vibration, 300 (3–5), pp.709–726.

[7] Yang, M., Hu, Y., Zhang, J., Ding, G., and Song, C., 2018. Analytical model for flexural damping responses of CFRP cantilever beams in the low-frequency vibration. *Journal of Low Frequency Noise Vibration and Active Control*, 37 (4), pp.669–681.

[8] Assie, A.E., Eltaher, M.A., and Mahmoud, F.F., 2011. Behavior of a viscoelastic composite plates under transient load. *Journal of Mechanical Science and Technology*, 25 (5), pp.1129–1140.

[9] Papanicolaou, G.C., Xepapadaki, A., Abiramia, G., and Jiga, G., 2008. Viscoelastic characterization of a glass - Epoxy composite. *Materiale Plastice*. 45 (3), pp.221–227.

[10] Naik, A., Abolfathi, N., Karami, G., and Ziejewski, M., 2008. Micromechanical viscoelastic characterization of fibrous composites. *Journal of Composite Materials*. 42 (12), pp.1179–1204.

[11] Vinogradov, A.M., 1985. Nonlinear effects in creep buckling analysis of column. *Journal of Engineering Mechanics*. 111 (6), pp.757–767.

[12] Shalev, D., and Aboudi, J., 1991. Postbuckling Analysis of Viscoelastic Laminated Plates Using Higher-order Theory. *International Journal of Solids and Structures*, 27(14), pp.1747-1755.

[13] Marques, S.P.C. and Creust, G.J., 1994. Geometrically Nonlinear Finite Element Analysis of Viscoelastic Composite Materials Under Mechanical and hygrothermal Loads. *Computers and Structures,* 53 (2), pp.449-456.

[14] Fung, R.F., Huang, J.S., and Chen, W.H., 1996. Dynamic stability of a viscoelastic beam subjected to harmonic and parametric excitations simultaneously. *Journal of Sound and Vibration*, 198 (1), pp.1–16.

[15] Ghabussi, A., Habibi, M., NoormohammadiArani, O., Shavalipour, A., Moayedi, H., and Safarpour, H., 2021. Frequency characteristics of a viscoelastic graphene nanoplatelet–reinforced composite circular microplate. *JVC/Journal of Vibration and Control*. 27 (1–2), pp.101–118.

[16] Al-Furjan, M.S.H., Samimi-Sohrforozani, E., Habibi, M., Jung, D. won, and Safarpour, H., 2021. Vibrational characteristics of a higher-order laminated composite viscoelastic annular microplate via modified couple stress theory. *Composite Structures*. 257 113152.

[17] Fan, Y. and Wang, Y., 2021. The effect of negative Poisson's ratio on the low-velocity impact response of an auxetic nanocomposite laminate beam. *International Journal of Mechanics and Materials in Design*. 17 (1), pp.153–169.

[18] Fan, Y., Xiang, Y., and Shen, H.S., 2020. Nonlinear Dynamics of Temperature-Dependent FG-GRC Laminated Beams Resting on Visco-Pasternak Foundations. *International Journal of Structural Stability and Dynamics*. 20 (1),.

[19] Kaliske, M. and Rothert, H., 1997. Formulation and implementation of three-dimensional viscoelasticity at small and finite strains. *Computational Mechanics*, 19 (3), pp.228–239.

[20] Kim, T.W. and Kim, J.H., 2002. Nonlinear vibration of viscoelastic laminated composite plates. *International Journal of Solids and Structures*. 39 (10), pp.2857–2870.

[21] Cederbaum, G., Aboudi, J., and Elishakoff, I., 1991. Dynamic instability of shear-deformable viscoelastic laminated plates by lyapunov exponents. *International Journal of Solids and Structures*, 28 (3), pp.317–327.

[22] Akay, H.U., 1980. Dynamic large deflection analysis of plates using mixed finite elements. *Computers and Structures*, 11 (1–2), pp.1–11.

[23] Sun, M., Chang, M., Wang, Z., Li, H., and Sun, X., 2018. Experimental and simulation study of low-velocity impact on glass fiber composite laminates with reinforcing shape memory alloys at different layer positions. *Applied Sciences (Switzerland)*, 8 (12).

[24] Shokrgozar, M., Tizfahm, A., and Mozaffari, A., 2021. Finite element analysis of viscoelastic laminates embedded with shape-memory-alloy wires under low-velocity impact considering large deflection. *Mechanics of Materials*. 156 , 103810.